

## Corner wetting in the two-dimensional Ising model: Monte Carlo results

This article has been downloaded from IOPscience. Please scroll down to see the full text article.

2003 J. Phys.: Condens. Matter 15 333

(<http://iopscience.iop.org/0953-8984/15/3/302>)

View [the table of contents for this issue](#), or go to the [journal homepage](#) for more

### Download details:

IP Address: 171.66.16.119

The article was downloaded on 19/05/2010 at 06:28

Please note that [terms and conditions apply](#).

## Corner wetting in the two-dimensional Ising model: Monte Carlo results

E V Albano<sup>1,2</sup>, A De Virgiliis<sup>1</sup>, M Müller<sup>2</sup> and K Binder<sup>2</sup>

<sup>1</sup> INIFTA, Universidad Nacional de La Plata, CC 16 Suc. 4, 1900 La Plata, Argentina

<sup>2</sup> Institut für Physik, Johannes Gutenberg Universität, Staudinger Weg 7, D-55099 Mainz, Germany

Received 31 October 2002

Published 13 January 2003

Online at [stacks.iop.org/JPhysCM/15/333](http://stacks.iop.org/JPhysCM/15/333)

### Abstract

Square  $L \times L$  ( $L = 24$ – $128$ ) Ising lattices with nearest neighbour ferromagnetic exchange are considered using free boundary conditions at which boundary magnetic fields  $\pm h$  are applied, i.e., at the two boundary rows ending at the lower left corner a field  $+h$  acts, while at the two boundary rows ending at the upper right corner a field  $-h$  acts. For temperatures  $T$  less than the critical temperature  $T_c$  of the bulk, this boundary condition leads to the formation of two domains with opposite orientations of the magnetization direction, separated by an interface which for  $T$  larger than the filling transition temperature  $T_f(h)$  runs from the upper left corner to the lower right corner, while for  $T < T_f(h)$  this interface is localized either close to the lower left corner or close to the upper right corner. Numerous theoretical predictions for the critical behaviour of this ‘corner wetting’ or ‘wedge filling’ transition are tested by Monte Carlo simulations. In particular, it is shown that for  $T = T_f(h)$  the magnetization profile  $m(z)$  in the  $z$ -direction normal to the interface is simply linear and the interfacial width scales as  $w \propto L$ , while for  $T > T_f(h)$  it scales as  $w \propto \sqrt{L}$ . The distribution  $P(\ell)$  of the interface position  $\ell$  (measured along the  $z$ -direction from the corners) decays exponentially for  $T < T_f(h)$  from either corner, is essentially flat for  $T = T_f(h)$  and is a Gaussian centred at the middle of the diagonal for  $T > T_f(h)$ . Furthermore, the Monte Carlo data are compatible with  $\langle \ell \rangle \propto (T_f(h) - T)^{-1}$  and a finite size scaling of the total magnetization according to  $M(L, T) = \tilde{M}\{(1 - T/T_f(h))^{v_\perp} L\}$  with  $v_\perp = 1$ . Unlike the findings for critical wetting in the thin film geometry of the Ising model, the Monte Carlo results for corner wetting are in very good agreement with the theoretical predictions.

(Some figures in this article are in colour only in the electronic version)

## 1. Introduction

It was pointed out 25 years ago that one may have a thermodynamic surface transition (=singularity of the surface excess free energy associated with a wall confining a semi-infinite fluid at gas–liquid coexistence, or related systems) from a ‘nonwet’ to a ‘wet’ state of a surface [1, 2]. Since then the possibility of a second order wetting transition and the associated critical behaviour for wetting with short range surface forces has attracted enormous theoretical attention [3–15], although the conditions to observe this phenomenon in the laboratory are very restrictive [16, 17]. However, both experiments [16, 17] and simulations [12–15] could only observe mean field critical behaviour, the interesting nontrivial critical exponents predicted by renormalization group methods [7–11] could not be verified and to date the reasons for this discrepancy are not entirely clear [6]. The situation is somewhat better for the case of the semi-infinite Ising square lattice with a free boundary at  $x = 0$ , where then a boundary field  $h$  is applied: the exact solution of Abraham *et al* [18–20] allows us to locate the line  $h = h_c(T)$  at which the critical wetting transition occurs exactly, and to obtain also the associated critical exponents ( $\beta_s = 1$ ,  $\nu_\perp = 1$ ,  $\nu_\parallel = 2$ ). These exponents characterize how the interface distance  $\langle \ell \rangle$  unbinds from the wall  $\{\langle \ell \rangle \propto (h_c(T) - h)^{-\beta_s}\}$  and the correlation length of interfacial fluctuations  $\xi_\perp$ ,  $\xi_\parallel$  in the directions perpendicular and parallel to the interface, respectively  $\{\xi_\perp \propto (h_c(T) - h)^{-\nu_\perp}$ ,  $\xi_\parallel \propto (h_c(T) - h)^{-\nu_\parallel}\}$ . However Monte Carlo simulations found that also in this model the range of  $|h_c(T) - h|$  where these exponents actually can be observed is extremely small [21].

Very recently it was pointed out [22–25] that the filling transition of wedges in  $d = 3$  dimensions [26–28] or the two-dimensional counterpart of corner wetting [29–33] provide further possibilities to study critical wetting. In particular, the critical exponents describing corner wetting are also believed to be known exactly, and for a rectangular corner the critical line  $h_c(T)$  is also known [31]

$$\cosh(2h_c(T)/k_B T) = \cosh(2J/k_B T) - \exp(-2J/k_B T) \sinh^2(2J/k_B T). \quad (1)$$

While this result for low temperatures also is compatible with calculations in the solid-on-solid approximation [34, 35], we are not aware of any extensive numerical tests of the predicted critical behaviour for this corner wetting transition yet.

Hence the present paper intends to fill this gap, presenting the first Monte Carlo study of corner wetting in the two-dimensional Ising square, including a discussion on how this transition shows up in a finite size scaling context [36]. Section 2 will briefly summarize the theoretical predictions on the critical behaviour that will be tested, while section 3 presents the Monte Carlo results. A brief summary is then given in section 4.

## 2. Theoretical background

The geometry of the Ising square lattice and its boundary conditions that are considered here is sketched in figure 1. We consider temperatures  $T < T_c$ , the critical temperature of the Ising model in the bulk two-dimensional geometry, and a strength  $h$  of the boundary fields  $\pm h$  applied in figure 1 less than the critical field  $h_c(T)$  (that is believed to be known exactly and is given by equation (1)). In the limit  $L \rightarrow \infty$  there will be a spontaneous magnetization in the system, which may be either positive or negative (the latter case is assumed in figure 1), and an interface will be present at an average distance  $\langle \ell_0 \rangle$  in the  $z$ -direction (figure 1). In the case where the spontaneous magnetization has the opposite sign, the interface will be at a distance  $\langle \ell_0 \rangle$  from the upper right corner rather than from the lower left corner ( $x = 0$ ,  $y = 0$ ), of course, since there is a perfect symmetry with respect to the sign of the total magnetization of the system present.

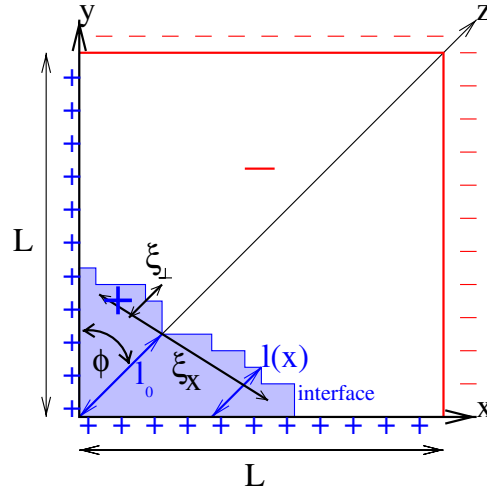


**Figure 1.** Simulation geometry of the  $L \times L$  Ising square lattice. Free boundary conditions are used for the spins in rows  $n_x = 1, n_x = L, n_y = 1$  and  $n_y = L$ , with the integers  $(n_x, n_y) \in [1, L]$  labelling the lattice sites. In addition, on all spins in the rows  $n_x = 1$  and  $n_y = 1$  acts a field  $h$ ; on all spins in the rows  $n_x = L$  and  $n_y = L$  acts a field  $-h$ . A typical configuration of the system for  $T < T_c$  then contains an interface running on average normal to the  $z$ -direction from some point in the row  $n_y = 1$  to a point in the row  $n_x = 1$  at the system boundaries, separating a domain of positive magnetization (+) from a domain with negative magnetization (-). The distance of the interface from the lower left corner is denoted by  $\ell_0$ . Fluctuations of the interface are characterized by correlation lengths  $\xi_x$  and  $\xi_\perp$  in the directions parallel and perpendicular to the interface, respectively.

The theory of corner wetting (or wedge filling, respectively) asserts that the transition occurs when the contact angle  $\Theta$  (describing droplets on a planar interface in the regime of incomplete wetting) satisfies the equation

$$\Theta(h_c(T)) = \pi/2 - \phi \quad (2)$$

where  $\phi$  is the angle that the wedge makes with the  $z$ -direction (figure 1). In our case  $\phi = \pi/4$ , of course. For the present model the transition is of second order and hence one expects power law divergences of both the mean distance  $\langle \ell_0 \rangle$  of the interface in the  $z$ -direction from the corner to which it is bound, and the parallel ( $\xi_x$ ) and perpendicular ( $\xi_\perp$ ) correlation lengths describing the fluctuations of the actual interface height  $\ell_0 = \ell(x = 0)$  in the directions parallel and perpendicular to the interface, respectively [29–33],

$$\langle \ell_0 \rangle \propto t^{-\beta_s}, \quad \xi_\perp \propto t^{-\nu_\perp}, \quad \xi_x \propto t^{-\nu_x}, \quad t = h_c(T) - h, \quad (3)$$

and the predicted critical exponents take the values

$$\beta_s = 1, \quad \nu_\perp = 1, \quad \text{and} \quad \nu_x = 1. \quad (4)$$

The probability distribution of the interface height takes the general form

$$P(\ell_0, t) \propto \frac{1}{\langle \ell_0 \rangle} \mathcal{P}\left(\frac{\ell_0}{\langle \ell_0 \rangle}, \frac{\xi_\perp}{\langle \ell_0 \rangle}\right). \quad (5)$$

Interestingly, the last argument can be omitted in the vicinity of the transition because both the mean value  $\langle \ell_0 \rangle$  of the interface from the corner to which it is bound and its fluctuation

$\xi_{\perp}$  diverge with the same exponent. Moreover, for small enough  $t$  the distribution of  $\ell_0$  is predicted to be a simple exponential,

$$P(\ell_0) = \frac{1}{\langle \ell_0 \rangle} \exp\left(-\frac{\ell_0}{\langle \ell_0 \rangle}\right), \quad t \rightarrow 0^+. \quad (6)$$

Of course, all these results, equations (3)–(6), apply when we first take the limit  $L \rightarrow \infty$  and the limit  $t \rightarrow 0$  afterwards. It is also of interest to ask what happens when the limits are taken in the inverse order. Then, Parry *et al* [30] predict that

$$P(\ell_0, t = 0) = \frac{1}{L}, \quad L \rightarrow \infty, \quad (7)$$

and the magnetization profile  $m(z)$  along the  $z$  axis is simply a straight line,

$$m(z) = m_b \left(1 - \frac{2z}{L}\right), \quad t = 0, L \rightarrow \infty, 0 \leq z \leq L. \quad (8)$$

In equations (7) and (8) we have chosen  $\sqrt{2}$  as the length unit in the  $z$ -direction (the actual distance between the lower left corner and the upper right corner is  $\sqrt{2}L$  lattice spacings, of course), and  $m_b$  is the spontaneous magnetization of an Ising model in the bulk at the considered temperature. It is also clear that for large  $L$  equation (6) also needs to be symmetrized with respect to both corners to which the interface can be bound, i.e.,

$$P(\ell_0) = \frac{1}{2\langle \ell_0 \rangle} \left\{ \exp\left(-\frac{\ell}{\langle \ell_0 \rangle}\right) + \exp\left(-\frac{[L - \ell_0]}{\langle \ell_0 \rangle}\right) \right\}. \quad (9)$$

Equation (9) is supposed to hold for  $t \rightarrow 0^+$ , i.e., in the region of incomplete corner wetting. In the opposite regime,  $t < 0$ , the average location of the interface is a straight line running from the upper left corner to the lower right corner, and hence

$$\langle \ell_0 \rangle = L/2 \quad \text{and} \quad P(\ell_0) \propto \exp\left(-\frac{[\ell_0 - \langle \ell_0 \rangle]^2}{2\xi_{\perp}^2}\right) \quad (10)$$

with [31]

$$\xi_{\perp} \propto L^{1/2}. \quad (11)$$

It is also of interest to consider the distribution  $\tilde{P}(m)$  of the magnetization of the Ising square with the boundary conditions specified by figure 1. For  $t < 0$  the result that the average location of the interface is the straight line normal to the  $z$ -direction connecting the corners of the square implies that the average magnetization  $\langle m \rangle = 0$ , and the Gaussian distribution to  $\ell_0$  translates into a Gaussian distribution of the magnetization,

$$\tilde{P}(m) \propto \exp\left(-\frac{m^2 L^2}{2k_B T \chi_L}\right) \quad \text{with} \quad \chi_L \propto \xi_{\perp}^2 \propto L. \quad (12)$$

Similar to the interface localization transition for the slit geometry [37–39], in the case  $t < 0$  where the interface is not bound to a wall (or a corner, respectively) one is in a ‘soft mode’ phase where both correlation lengths ( $\xi_{\parallel} \propto L$ ,  $\xi_{\perp} \propto L^{1/2}$ ) and the susceptibility  $\chi_L$  diverge as  $L \rightarrow \infty$ . Note that equation (11) can simply be interpreted in terms of a random walk description of an interface in  $d = 2$  dimensions, where excursions in normal direction to the average interface orientation add up randomly [40].

It is useful to relate the interface position  $\ell_0$  to the magnetization. For  $t > 0$  the interface is bound to the lower left corner at a distance  $\langle \ell_0 \rangle$ . Given the complete interface configuration  $\ell(x)$  we can calculate the magnetization via

$$m[\ell(x)] = -m_b \left(1 - \frac{2}{L^2} \int_0^L dx \ell(x)\right). \quad (13)$$

Of course, even the average interface configuration only becomes a straight line normal to the  $z$ -axis in the limit  $t \rightarrow 0$ , while it is curved towards the corner for positive  $t$ . Nevertheless, in the vicinity of the corner wetting transition, we can approximate the magnetization by

$$m \approx -m_b \left( 1 - 2 \frac{\ell_0^2}{L^2} \right), \quad L \rightarrow \infty. \quad (14)$$

In the following we rather work with the absolute value  $|m|$  of the magnetization, because states with positive and negative magnetization are equally probable, depending on to which corner the interface is bound. The probability distribution  $P(\ell_0)$  then yields an approximation for the probability distribution of the magnetization

$$\tilde{P}(|m|) \approx \frac{L}{2m_b \sqrt{2(1 - |m|/m_b)}} P\left(\ell_0 = L\sqrt{(1 - |m|/m_b)/2}\right). \quad (15)$$

Note that in this approximation  $\tilde{P}(m)$  has an integrable singularity at  $m = \pm m_b$ . If equation (14) were correct those values of the magnetization would correspond to the extreme values  $\ell_0 = 0$  or  $L$ . Clearly, equation (13) breaks down in this limit, because there are microscopic enrichment layers at the surfaces which prevent the magnetization from adopting those limiting values. Nevertheless, we expect the probability distribution of the magnetization to be strongly peaked for  $t \geq 0$ .

Right at the transition ( $t = 0$ ), the probability distribution of  $\ell_0$  is flat (cf equation (7)) and equation (15) yields  $\langle |m| \rangle \approx 2m_b/3$ . Although this is not meant as an exact result, it already suggests a finite size scaling structure of the magnetization  $\langle m \rangle$ . We assume a dependence on  $L/\langle \ell_0 \rangle$  or—since  $\langle \ell_0 \rangle$  and  $\xi_\perp$  have the same exponent—on  $L/\xi_\perp$ . Thus, we conclude that  $\langle |m| \rangle$  should scale as follows:

$$\langle |m| \rangle = m_b \tilde{m}(L/\xi_\perp) = m_b \tilde{m}(Lt), \quad L \rightarrow \infty, t \rightarrow 0, |Lt| \text{ finite}, \quad (16)$$

where we have used the prediction that  $v_\perp = 1$ .

Note that unlike critical phenomena in the bulk, where a scaling power  $L^{-\beta/\nu}$  appears when  $\beta$  is a nontrivial order parameter exponent [41], no such scaling power appears here. This result is intuitively clear from geometric reasons (and also obvious from equation (14)): when we consider the limit  $L \rightarrow \infty$  at fixed  $t > 0$  on the one hand, we obtain  $\langle m \rangle = \pm m_b$ , because the correction due to the oppositely magnetized domain in one of the corners becomes negligibly small,  $\langle \ell_0 \rangle$  staying finite when  $L \rightarrow \infty$ . In this sense we asymptotically have a transition where the magnetization of the Ising lattice vanishes discontinuously at  $t \rightarrow 0$  when the limit  $L \rightarrow \infty$  is taken first. On the other hand, for any finite  $L$  this transition is clearly rounded. Already for  $t > 0$  there is a finite nonzero probability that  $m = 0$  in the Ising square occurs, and there is no spontaneous symmetry breaking.

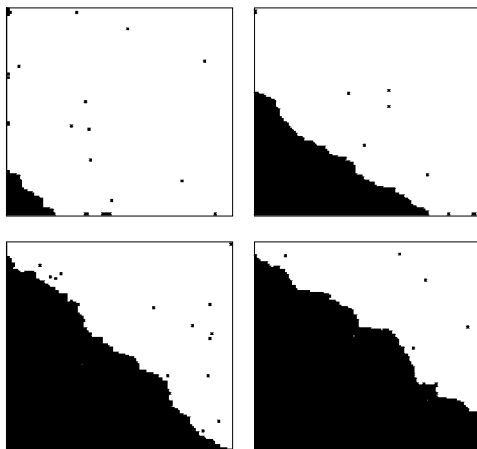
Analogous arguments suggest a related scaling for the susceptibility of the finite square

$$k_B T \chi = L^2 (\langle m^2 \rangle - \langle |m| \rangle^2) = L^2 \tilde{\chi}(Lt). \quad (17)$$

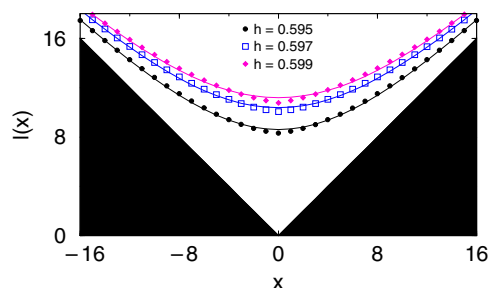
### 3. Numerical results

Standard single-spin-flip Monte Carlo runs using the Metropolis algorithm [42–44] have been performed. We vary the system size  $L$  from 32 to 128. Averages were taken over runs of  $1 \times 10^6$ – $2 \times 10^6$  Monte Carlo steps/spin (MCS) duration, after discarding  $1 \times 10^5$ – $2 \times 10^5$  MCS for equilibrium. In order to improve the statistics, we made up to eight independent runs for each of the parameters studied.

Figure 2 shows typical snapshots of the system configuration. One sees qualitatively the expected behaviour: for  $h = 0.60$  (i.e.,  $t > 0$ ) the interface is clearly localized close to a corner



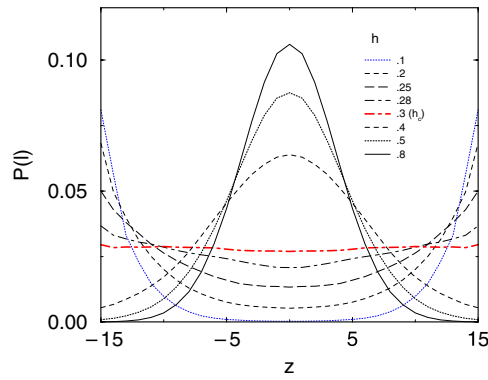
**Figure 2.** Snapshot pictures for  $L = 128$ ,  $T = 0.5$  (in units of the bulk critical temperature) and for different fields  $h$  (in units of  $J$ ):  $h = 0.60, 0.61, 0.62$  and  $0.63$ . Note, however, that the critical field occurs at  $h_c = 0.606$ . Up spins are represented by black squares, while down spins are left white.



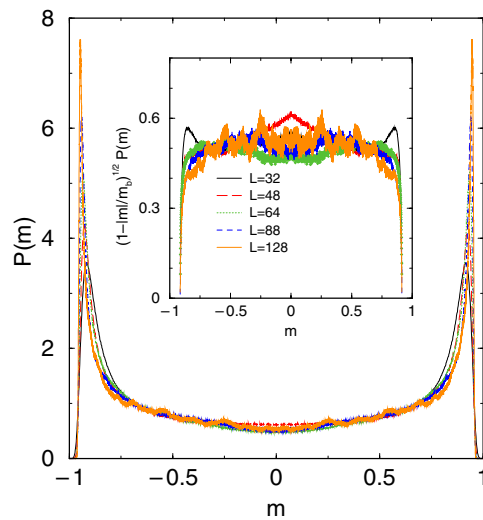
**Figure 3.** Average interface position for  $L = 64$  and  $T = 0.5$ . The values of the magnetic field  $h < h_c$  are indicated in the key. Symbols refer to Monte Carlo data, while the curves present fits according to  $l(x) = A + B \ln[1 + C \exp(x/D) + C \exp(-x/D)]$  with four parameters  $A, B, C, D$ . We have rotated the  $x$ -axis by  $45^\circ$  compared to figure 1, in order to use the same notation as in [22].

of the square, while in the other cases the distance  $\ell_0$  of the interface from either corner is rather large. Of course, the interface position is strongly fluctuating, and also for  $L = 128$  the corner wetting transition is clearly affected by finite size rounding effects. Therefore an inspection of snapshot pictures cannot suffice for a quantitative characterization of the transition, and a more detailed analysis is required.

The average location of the interface in the wedge for the same temperature as above and  $h < h_c$  is shown in figure 3. Qualitatively, the interface position can be fitted by an expression of the form  $l(x) = A + B \ln[1 + C \exp(x/D) + C \exp(-x/D)]$ , where  $A, B, C$  and  $D$  are fitting parameters. This functional form is suggested by mean field calculations using an effective interface Hamiltonian [22]. Compared to figure 1 the  $x$ -axis is rotated by  $45^\circ$  in accord with [22] (cf figure 3). With four free fitting parameters, however, we cannot obtain perfect agreement with our Monte Carlo data. This might point to important fluctuation effects, which are not accounted for in the mean field treatment. The figure also reveals the deficiency of approximation (14), which relates the magnetization to the distance  $l_0$ .



**Figure 4.** Probability distribution  $P(\ell_0)$  of the interface position along the  $z$ -direction for  $T = 0.85$ ,  $L = 32$ , and eight different fields  $h$  as indicated in the figure (note that  $h_c(T) \approx 0.3$  here).



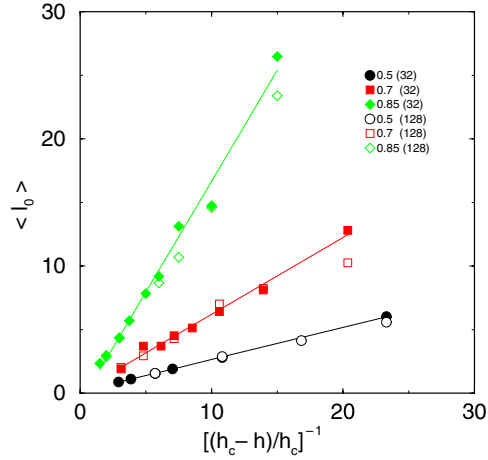
**Figure 5.** Probability distribution of the magnetization at the filling transition  $h = 0.375$ . The inset plots the data with the factor  $\sqrt{1 - |m|/m_b}$  with  $m_b = 0.914$  as suggested by equation (15).

Figure 4 now presents the probability distribution  $P(\ell_0)$  of the interface position, in order to provide a first test of equations (7), (9) and (10): indeed one can nicely see the exponential decays near the corners for  $t > 0$  (cf equation (9)), the essentially flat behaviour of  $P(\ell_0)$  for  $t = 0$  (cf equation (7)) and the Gaussian behaviour for  $t < 0$  (cf equation (10)).

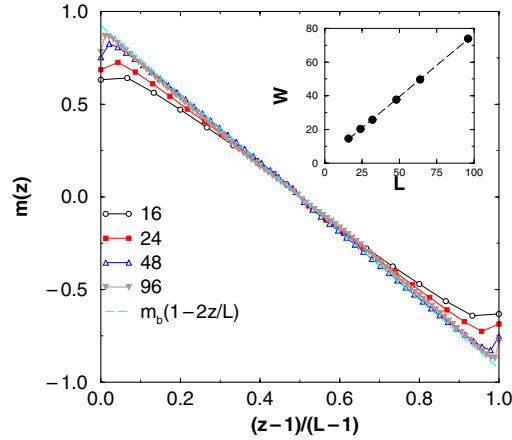
The probability distribution of the magnetization is presented in figure 5. The distribution at the filling transition is indeed independent of the system size. The distribution shows pronounced peaks near to  $m = \pm m_b \approx \pm 1$ , and the singularity can be much reduced by multiplying the data by the factor  $\sqrt{1 - |m|/m_b}$  as suggested by equation (15). Except for the vicinity of the boundaries  $m = \pm m_b$  the function  $\sqrt{1 - |m|/m_b}P(m)$  is rather flat, which corresponds to a flat distribution of  $l$  as shown in figure 4. The typical frequency of transitions between the two equivalent interface positions is proportional to  $P(m = 0)$ .

Figure 6 then tests the predicted divergence of  $\langle \ell_0 \rangle$  as  $t \rightarrow 0$ . Again the predicted behaviour  $\langle \ell_0 \rangle \propto t^{-1}$  according to equation (3) is straightforwardly verified.





**Figure 6.** Interface position  $\langle \ell_0 \rangle$  plotted versus  $\{[h_c(T) - h]/h_c(T)\}^{-1}$ , for three different temperatures:  $T = 0.5$  (circles),  $0.7$  (squares) and  $0.85$  (diamonds). Filled symbols refer to  $L = 32$ ; open symbols refer to  $L = 128$ . For  $h_c(T)$  the theoretical values from equation (1) were used.



**Figure 7.** Normalized magnetization profiles  $m(z)$  versus  $(z-1)/(L-1)$  for four different choices of  $L$  at  $T = 0.75$  and  $h = h_c(T) = 0.4$ . The broken line displays the asymptotic result, equation (8). Note that the abscissa variable is used to convert the integer indices for lattice coordinates  $1, 2, \dots, L$  to a continuous variable in the interval from zero to unity, irrespective to the choice of  $L$ . The inset shows a linear plot of the width  $W$  versus  $L$ , to demonstrate the linear variation.

Also the expected linear variation of the magnetization profile along the diagonal for  $t = 0$  is clearly seen in our simulations, and the approach to the asymptotic formula equation (8) as  $L$  increases is rather rapid. Indeed, at  $t = 0$  the width  $W$  of the magnetization profile scales linearly with  $L$ , as it should (cf figure 7 inset). In contrast, if we are in the region where the interface is no longer bound to a corner, the magnetization profile is not at all linear (cf figure 8). In fact, it can rather be fitted to a tanh-function, and from the slope at the midpoint ( $dm(z)/dz$  at the point where  $m(z) = 0$ ) we again extract  $W$ . The inset shows that the prediction  $W \propto L^{1/2}$  (cf equation (11)) is well confirmed.

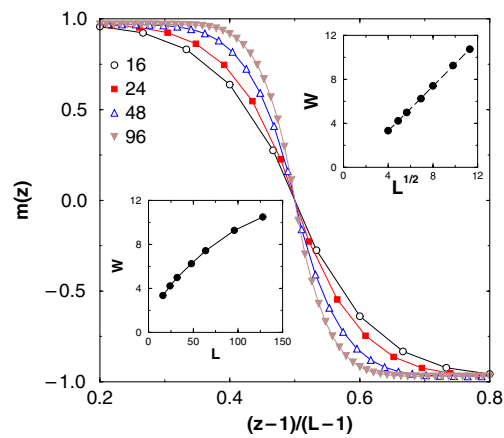


**Figure 8.** The same as figure 7, but for  $h = 1.0$ . The insets show  $W$  versus  $L$  in a linear-linear plot (lower inset) and in the form  $W$  versus  $L^{1/2}$  (upper inset).

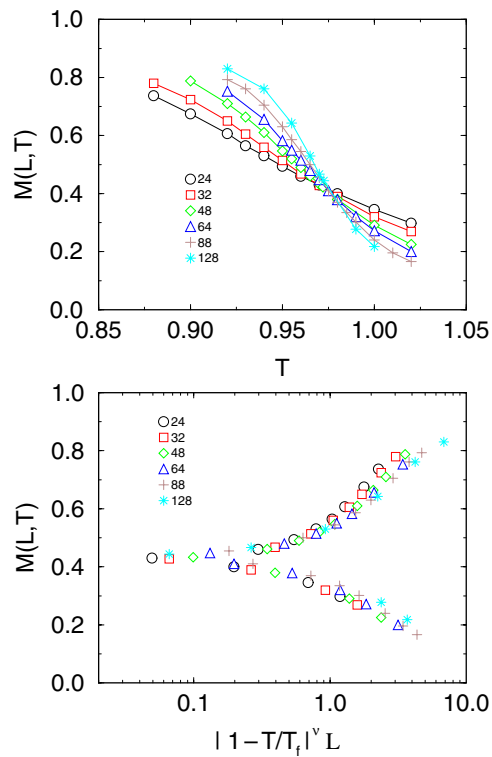


**Figure 9.** Absolute value of the total magnetization  $M(L, T) \equiv \langle |m| \rangle$  plotted versus temperature for  $h = 0.125$  (upper part) and data rescaled against the scaling variable  $|1 - T/T_f(h)|^{\nu_{\perp}} L = |1 - T/T_f|L$  (lower part). Linear dimensions  $L$  ranging from 24 to 128 are included, as indicated.

Next we turn to the analysis of the total magnetization. Figures 9–12 present the results for different surface fields. Note that we can either approach the corner wetting transition by

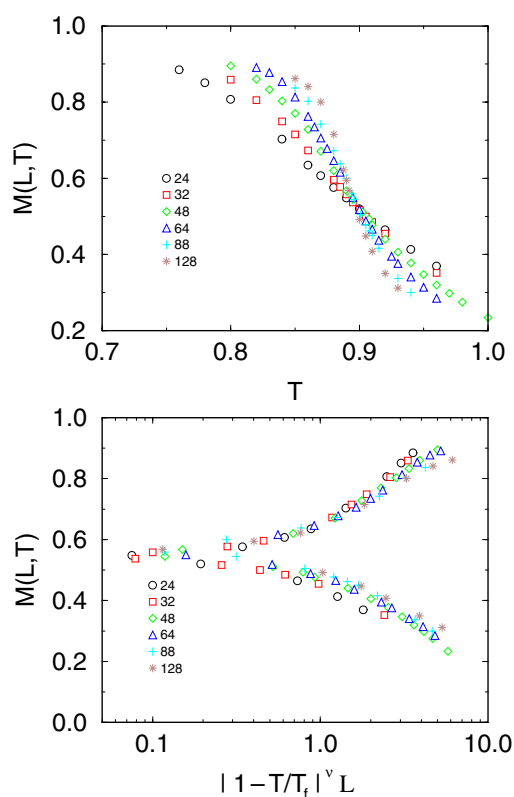


**Figure 10.** The same as figure 9, but for  $h = 0.25$ .

varying  $T$  at fixed  $h$  (as done in figures 9–11) or by varying the surface field  $h$  at fixed  $T$  (as done in figure 12). Then the transition line  $T = T_f(h)$  simply denotes the inverse function of  $h = h_c(T)$ . Since there is no power of  $L$  prefactor in equation (16), this equation implies that for  $t = 0$  all curves  $M(L, T)$  versus  $T$  should intersect in a common intersection point, independent of  $L$ , and this indeed is verified. Actually, the value of the magnetization at this intersection point  $\langle |m| \rangle / m_b$  is around 0.75.

Finally, in figure 13 we present a scaling plot of the susceptibility at low temperatures (a) and closer to the bulk critical point (b). Again the Monte Carlo data are compatible with the predicted scaling behaviour in equation (17), although it is difficult to obtain good statistics for this quantity at low temperatures due to protracted long correlation times.

#### 4. Summary

We have presented an extensive Monte Carlo study of corner wetting in two dimensions. The two-dimensional case poses a rather stringent test on the theory of Parry *et al* [29–33] because there are detailed predictions not only for the critical exponents but also for the scaling functions. Moreover, the simulations are facilitated by the exact knowledge of the location of the transition in the thermodynamic limit, and rather large systems are accessible to simulations in two dimensions. In contrast to critical wetting on planar substrates [12–17], our Monte Carlo results do corroborate the theoretical prediction. Most notably, we confirm the value of the

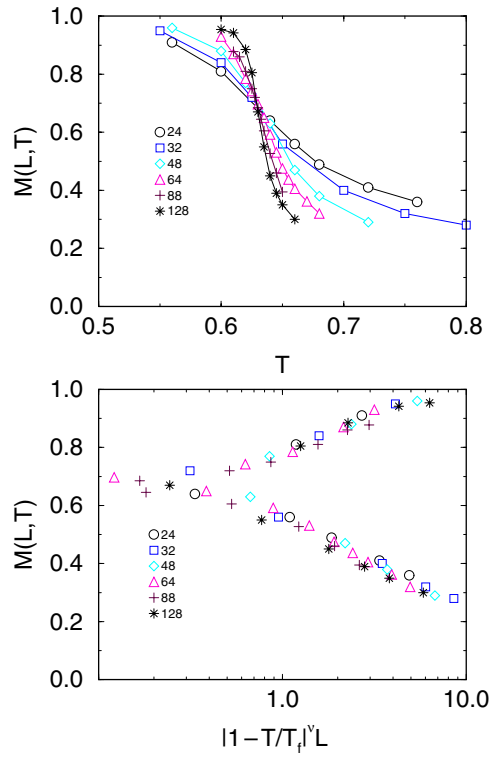
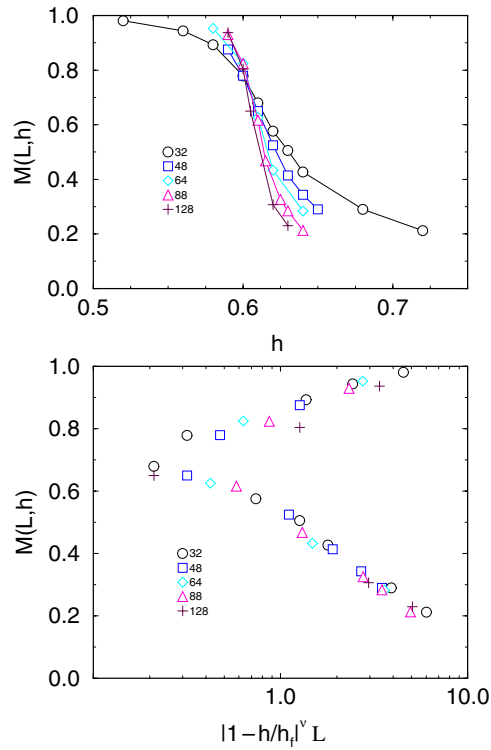


Figure 11. The same as figure 9, but for  $h = 0.5$ .

critical exponents  $\beta_0 = \nu_\perp = 1$ . It would also be interesting to test the predictions in the case where the opening angle tends towards  $\pi$ ; in this limit we would gradually approach critical wetting on a planar substrate.

Additionally, the simulations reveal rather pronounced finite size effects, which set in already when the distance of the interface  $\ell_0$  from the corner is a finite (and rather small) fraction of the system size. We employ a naive mapping between the distance  $\ell_0$  and the order parameter, the total magnetization  $m$  of the square. While this is sufficient to motivate the finite size scaling of the order parameter, we also observe deviations from this naive approach. For instance, at the transition the probability distribution of  $\ell_0$  is uniform and our naive mapping suggests that the magnetization adopts the value  $2m_b/3$ . While the independence of this value from the system size is supported by our Monte Carlo data, the actual value is somewhat larger. A quantitative relation between the probability distribution of  $\ell_0$  and the order parameter requires knowledge of the entire interface configuration. We have presented the Monte Carlo data of this quantity, but a theoretical prediction which takes due account of fluctuations is—to the best of our knowledge—not available.

Our simulations have been restricted to temperatures not too close to the bulk critical point in order to separate the effects of wetting and bulk criticality. For even smaller surface fields, the corner wetting transition gradually approaches the bulk critical point, and we anticipate a rich interplay between both phenomena.



**Figure 12.** Absolute value of the total magnetization  $M(L, h) \equiv \langle |m| \rangle$  plotted versus field for  $T = 0.5$  (upper part) and data rescaled against the scaling variable  $|1 - h/h_c(T)|L$  (lower part).

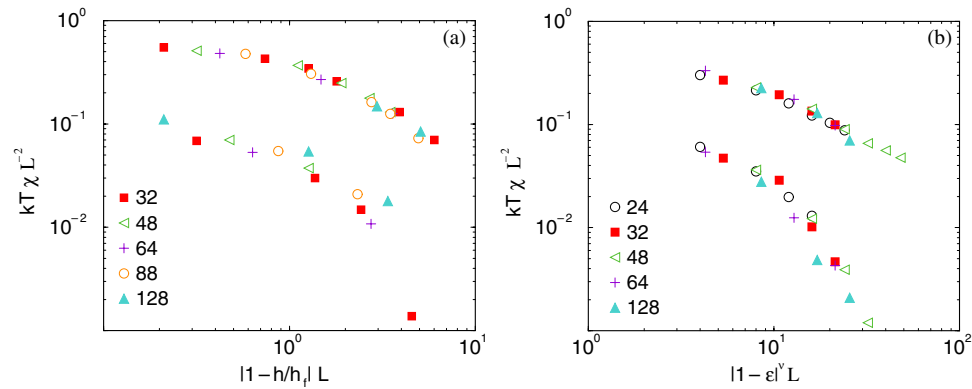


**Figure 13.** Scaling plot of the susceptibility  $\chi(t < 0)$  or  $\chi'(t > 0)$  versus  $|t|L$ , for the case  $T = 0.5$  (a) and the case  $T = 0.85$  (b). Note that  $k_B T \chi = \langle m^2 \rangle L^2$ ,  $k_B T \chi' \equiv (\langle m^2 \rangle - \langle |m| \rangle^2) L^2$  is used [44]. Linear dimensions from  $L = 32$  to  $128$  are included, as indicated in the figure.

## Acknowledgments

EVA was supported by the Alexander von Humboldt foundation. AV received financial support from the DAAD/PROALAR2000. MM thanks the DFG for a Heisenberg stipend. Partial support by the DFG in the framework of the priority programme ‘Wetting and structure formation at interfaces’ (Bi314-17) is gratefully acknowledged.

## References

- [1] Cahn J W 1977 *J. Chem. Phys.* **66** 3667
- [2] Ebner C and Saam W F 1977 *Phys. Rev. Lett.* **38** 1486
- [3] Dietrich S 1988 *Phase Transitions and Critical Phenomena* vol 12, ed C Domb and J L Lebowitz (London: Academic) p 1
- [4] Schick M 1990 *Liquids at Interfaces (Les Houches, Session XLV III)* ed J Charvolin, J F Joanny and J Zinn-Justin (Amsterdam: Elsevier) p 415
- [5] Forgacs G, Lipowsky R and Nieuwenhuizen Th M 1991 *Phase Transitions and Critical Phenomena* vol 14, ed C Domb and J L Lebowitz (London: Academic) p 135
- [6] Parry A O 1996 *J. Phys.: Condens. Matter* **8** 10761
- [7] Brézin E, Halperin B I and Leibler S 1983 *Phys. Rev. Lett.* **50** 1387
- [8] Brézin E, Halperin B I and Leibler S 1983 *J. Physique* **44** 775
- [9] Kroll D M, Lipowsky R and Zia R K P 1983 *Phys. Rev. B* **27** 1387
- [10] Lipowsky R 1985 *J. Phys. A: Math. Gen.* **18** L585  
Lipowsky R 1985 *Phys. Rev. B* **32** 1731
- [11] Lipowsky R and Fisher M E 1987 *Phys. Rev. B* **36** 2126
- [12] Binder K, Landau D P and Kroll D M 1986 *Phys. Rev. Lett.* **56** 2272
- [13] Binder K and Landau D P 1988 *Phys. Rev. B* **37** 1745
- [14] Binder K, Landau D P and Wansleben S 1989 *Phys. Rev. B* **40** 6971
- [15] Binder K, Landau D P and Müller M 2002 *J. Stat. Phys.* at press
- [16] Ross D, Bonn D and Meunier J 1999 *Nature* **400** 737
- [17] Ross D, Bonn D and Meunier J 2001 *J. Chem. Phys.* **114** 2784
- [18] Abraham D B 1980 *Phys. Rev. Lett.* **44** 1165
- [19] Abraham D B 1984 *Physica A* **124** 1  
Abraham D B and Smith E R 1986 *J. Stat. Phys.* **43** 621
- [20] Abraham D B 1988 *J. Phys. A: Math. Gen.* **21** 1741  
Upton P J 1999 *Phys. Rev. E* **60** R3475
- [21] Albano E V, Binder K, Heermann D W and Paul W 1990 *J. Stat. Phys.* **61** 161
- [22] Rejmer K, Dietrich S and Napiorkowski M 1999 *Phys. Rev. E* **60** 4027  
Rejmer K and Napiorkowski M 2000 *Phys. Rev. E* **62** 588
- [23] Parry A O, Rascon C and Wood A J 2000 *Phys. Rev. Lett.* **85** 345
- [24] Parry A O, Wood A J and Rascon C 2001 *J. Phys.: Condens. Matter* **13** 4591
- [25] Bednorz A and Napiorkowski M 2001 *J. Phys. A: Math. Gen.* **33** L353
- [26] Concus P and Finn R 1969 *Proc. Natl Acad. Sci. USA* **63** 292
- [27] Pomeau Y 1986 *J. Colloid Interface Sci.* **113** 5
- [28] Hauge E H 1992 *Phys. Rev. A* **46** 4994
- [29] Parry A O, Rascon C and Wood A J 1999 *Phys. Rev. Lett.* **83** 5535
- [30] Parry A O, Wood A J and Rascon C 2000 *J. Phys.: Condens. Matter* **12** 7671
- [31] Parry A O, Wood A J, Carlon E and Drzewinski A 2001 *Phys. Rev. Lett.* **87** 196103
- [32] Parry A O, Greenall M J and Wood A J 2002 *J. Phys.: Condens. Matter* **14** 1169
- [33] Abraham D B, Parry A O and Wood A J 2002 *Europhys. Lett.* **60** 106
- [34] Duxbury P M and Orrick A C 1989 *Phys. Rev. B* **39** 2944
- [35] Lipowski A 1998 *Phys. Rev. E* **58** R1
- [36] See  
Milchev A, Müller M, Binder K and Landau D P 2002 (*Preprint*) for a more detailed discussion of finite size scaling in the context of the wedge filling transition
- [37] Albano E V, Binder K and Heermann D W 1989 *Surf. Sci.* **223** 15
- [38] Parry A O and Evans R 1990 *Phys. Rev. Lett.* **64** 523
- [39] Parry A O and Evans R 1992 *Physica A* **181** 250
- [40] Fisher M E 1986 *J. Chem. Soc. Faraday Trans. II* **82** 1589
- [41] Binder K 1992 *Computational Methods in Field Theory* ed H Gausterer and C B Lang (Berlin: Springer) p 59
- [42] Binder K 1997 *Rep. Prog. Phys.* **60** 487
- [43] Landau D P and Binder K 2000 *A Guide to Monte Carlo Simulation in Statistical Physics* (Cambridge: Cambridge University Press)
- [44] Binder K and Heermann D W 2002 *Monte Carlo Simulation in Statistical Physics. An Introduction* 4th edn (Berlin: Springer)